optica

# Shearing interferometry via geometric phase: supplementary material

LUIS A. ALEMÁN-CASTANEDA[1], BRUNO PICCIRILLO[2,*], ENRICO SANTAMATO[2], LORENZO MARRUCCI[2,3], AND MIGUEL A. ALONSO[1,4,5]

[1] The Institute of Optics, University of Rochester, Rochester NY 14627, USA
[2] Dipartimento di Fisica "Ettore" Pancini, Università di Napoli Federico II, Complesso Universitario MSA, Napoli, Italy
[3] CNR-ISASI, Institute of Applied Science and Intelligent Systems, Via Campi Flegrei 34, Pozzuoli (NA), Italy
[4] Center for Coherence and Quantum Optics, University of Rochester, Rochester NY 14627, USA
[5] Aix-Marseille Univ., CNRS, Centrale Marseille, Institut Fresnel, UMR 7249, 13397 Marseille Cedex 20, France
[*] Corresponding author: bruno.piccirillo@unina.it

*Published 21 March 2019*

**This document provides supplementary information to "Shearing interferometry via geometric phase," https://doi.org/10.1364/OPTICA.6.000396. It presents a study of the extension of shearing interferometry through geometric phase to more general geometries, with the aim of showing the full potential of this technique. Any pair of identical SVAPs (introduced in the main body) conveniently displaced along the propagation direction, can be adopted to create two oppositely-deformed coherent replicas of the input beam. Since the SVAPs can be designed to reshape the input wavefront at will, more general geometries can be easily devised in addition to the linear and radial ones. We present a proof of this concept based on a ray-optical approach, accounting for higher order wave features. This analysis provides useful criteria for ensuring that setups analogous to those proposed in the main body are able to perform tailored directional derivatives with respect to general degrees of freedom.**

## 1. EFFECT OF ARBITRARY SVAP PAIRS

Let the incident linearly-polarized field be given by $\boldsymbol{E}(\boldsymbol{x},0) = E(\boldsymbol{x},0)\,(\boldsymbol{C}_+ + \boldsymbol{C}_-)\,/\sqrt{2}$, where $\boldsymbol{x} = (x,y)$ and $\boldsymbol{C}_\pm = (\boldsymbol{x} \pm i\boldsymbol{y})/\sqrt{2}$ are the two circular polarization basis vectors. This field then traverses two identical spatially varying axis birefringent plates (SVAPs), whose fast axes are oriented at angles $\Theta(\boldsymbol{x})$. The derivation that follows uses ray optics to model the field's amplitude and phase after the two SVAPs. Suppose that a ray is incident at the point $\boldsymbol{x}_0$ on the first SVAP, with transverse direction cosines $\boldsymbol{p}_0$ (also referred to as the optical momentum). After passing through the first SVAP, this direction acquires a shift whose sign depends on the handedness of the polarization in question, according to $\boldsymbol{p}_1 = \boldsymbol{p}_0 \pm \boldsymbol{\delta}(\boldsymbol{x}_0)$, where $\boldsymbol{\delta}(\boldsymbol{x}_0) = k^{-1}\nabla\Theta(\boldsymbol{x}_0)$, with $\nabla$ denoting the vector differential operator over the transverse plane. This is followed by free propagation by a distance $z$, which leaves the direction unchanged but changes the ray coordinates according to

$$\boldsymbol{x} = \boldsymbol{x}_0 + z\boldsymbol{p}_0 \pm z\boldsymbol{\delta}(\boldsymbol{x}_0). \tag{S1}$$

Finally, transmission through the second SVAP at $z = \zeta$ leaves the ray position unchanged but introduces a second direction shift that is nearly the opposite of the first:

$$\begin{aligned}\boldsymbol{p}_2 &= \boldsymbol{p}_1 \mp \boldsymbol{\delta}(\boldsymbol{x}) = \boldsymbol{p}_0 \pm \boldsymbol{\delta}(\boldsymbol{x}_0) \mp \boldsymbol{\delta}(\boldsymbol{x}) \\ &= \boldsymbol{p}_0 \pm \frac{1}{k}\left[\nabla\Theta(\boldsymbol{x}_0) - \nabla\Theta(\boldsymbol{x})\right] \\ &= \boldsymbol{p}_0 \pm \frac{1}{k}\left[\Delta_i\partial_i\nabla\Theta(\boldsymbol{x}) + \frac{1}{2}\Delta_i\Delta_j\partial_i\partial_j\nabla\Theta(\boldsymbol{x}) + \dots\right].\end{aligned} \tag{S2}$$

where we define $\boldsymbol{\Delta} = \boldsymbol{x}_0 - \boldsymbol{x}$, and use the convention of implicit sum over repeated indices in the last step, with $\partial_i = \{\nabla\}_i$. Except for special cases such as the $\Lambda$-plates discussed in the main body, the two momentum shifts do not exactly cancel due to the fact that the ray hits the second SVAP at a slightly different coordinate.

In order to express the residual direction in terms of the final coordinates $\boldsymbol{x}$, we need to find an expression for $\boldsymbol{\Delta}$ in terms of $\boldsymbol{x}$ by using Eq. (S1) at the second SVAP:

$$\boldsymbol{\Delta} = -\zeta\boldsymbol{p}_0 \mp \frac{\zeta}{k}\nabla\Theta(\boldsymbol{x} + \boldsymbol{\Delta}). \tag{S3}$$

Applying recursively this relation through a Taylor expansion, and dropping the explicit dependence on $\boldsymbol{x}$, we obtain

$$\boldsymbol{\Delta} \approx -\zeta \boldsymbol{p}_0 \mp \frac{\zeta}{k}\left(\nabla\Theta + \boldsymbol{\Delta}\cdot\mathbb{H}_\Theta\right) \tag{S4}$$

$$\approx -\zeta \boldsymbol{p}_0 \mp \frac{\zeta}{k}\nabla\Theta \pm \frac{\zeta^2}{k}\mathbf{p}_0\cdot\mathbb{H}_\Theta + \frac{\zeta^2}{k^2}\nabla\Theta\cdot\mathbb{H}_\Theta, \tag{S5}$$

where $\mathbb{H}_\Theta$ is the Hessian matrix of $\Theta$ with components $\{\mathbb{H}_\Theta\}_{ij} = \partial_i\partial_j\Theta$. Notice that we keep terms only up to second order in $\zeta/k = \zeta\lambda/2\pi$, which is a parameter with units of square length that naturally enters the equations and whose square root is assumed to be small compared to the scale of spatial variation of the SVAPs.

Substituting in Eq. (S2) we find that the final direction mismatch can be expressed as a gradient

$$\boldsymbol{p}_2 - \boldsymbol{p}_0 \approx \frac{1}{k}\nabla(\Phi_1 \pm \Phi_2), \tag{S6}$$

where

$$\Phi_1 = -\frac{\zeta}{k}\frac{|\nabla\Theta|^2}{2} + \frac{\zeta^2}{k}\boldsymbol{p}_0\cdot\mathbb{H}_\Theta\cdot\nabla\Theta, \tag{S7}$$

$$\Phi_2 = \frac{\zeta^2}{k^2}\frac{\nabla\Theta\cdot\mathbb{H}_\Theta\cdot\nabla\Theta}{2} - \zeta\boldsymbol{p}_0\cdot\nabla\Theta + \zeta^2\boldsymbol{p}_0\cdot\mathbb{H}_\Theta\cdot\boldsymbol{p}_0. \tag{S8}$$

In the substitution of Eqs. (S7) and (S8) into Eq. (S6) we take $\boldsymbol{p}_0$ to be independent of $\boldsymbol{x}$. The fact that the total direction change is proportional to a gradient is consistent with the fact that the rays constitute a normal congruence, namely, that they are solutions to an eikonal equation.

The field after the second SVAP can be expressed in terms of the nominal field (without the SVAPs) at $z = \zeta$ according to the following approximation:

$$\frac{\exp(i\Phi_1)}{\sqrt{2}}\Big[\sqrt{j_-}E\left(\boldsymbol{x}-\boldsymbol{\epsilon},\zeta\right)\exp(i\Phi_2)\mathbf{C}_+ + \sqrt{j_+}E\left(\boldsymbol{x}+\boldsymbol{\epsilon},\zeta\right)\exp(-i\Phi_2)\mathbf{C}_-\Big], \tag{S9}$$

where $\boldsymbol{\epsilon}(\boldsymbol{x}) = k^{-1}\zeta\nabla\Theta(\boldsymbol{x})$ and the Jacobians $j_\pm$, which guarantee power conservation, are defined as

$$j_\pm = \frac{\partial(\boldsymbol{x}\pm\boldsymbol{\epsilon})}{\partial(\boldsymbol{x})} = 1 \pm \frac{\zeta}{k}\nabla^2\Theta + \frac{\zeta^2}{k^2}\mathrm{Det}(\mathbb{H}_\Theta). \tag{S10}$$

By using the approximation $\sqrt{j_\pm} \approx 1 \pm k^{-1}\zeta\nabla^2\Theta/2$ and the shorthands $\mathcal{S} = E\left(\boldsymbol{x}+\boldsymbol{\epsilon},\zeta\right) + E\left(\boldsymbol{x}-\boldsymbol{\epsilon},\zeta\right)$, $\mathcal{D} = E\left(\boldsymbol{x}+\boldsymbol{\epsilon},\zeta\right) - E\left(\boldsymbol{x}-\boldsymbol{\epsilon},\zeta\right)$ and $a = k^{-1}\zeta\nabla^2\Theta/2$, the intensity measured after an analyzer oriented at an angle $\psi$ can be found to be

$$\begin{aligned} I(\psi) &\propto |(\mathcal{S}+a\mathcal{D})\cos(\psi+\Phi_2) + i(\mathcal{D}+a\mathcal{S})\sin(\psi+\Phi_2)|^2 \\ &= (|\mathcal{S}|^2 + a^2|\mathcal{D}|^2)\cos^2(\psi+\Phi_2) \\ &+ (|\mathcal{D}|^2 + a^2|\mathcal{S}|^2)\sin^2(\psi+\Phi_2) \\ &+ 2a\mathrm{Re}(\mathcal{S}^*\mathcal{D}) + (1-a^2)\mathrm{Im}(\mathcal{S}^*\mathcal{D})\sin[2(\psi+\Phi_2)]. \end{aligned} \tag{S11}$$

In the limit of small shears, we can approximate $\mathcal{S} \approx 2E$ and $\mathcal{D} \approx 2\boldsymbol{\epsilon}\cdot\nabla E$. Also, under some conditions to be discussed later, we can ignore $\Phi_2$, to get

$$\begin{aligned} I(\psi) \mathrel{\tilde{\propto}} &|E|^2\cos^2\psi + \frac{\zeta}{k}|E|^2\nabla\Theta\cdot\nabla\mathrm{Arg}(E)\sin 2\psi \\ &+ \frac{\zeta^2}{4k^2}\Big\{\Big[4|\nabla\Theta\cdot\nabla E|^2 + (\nabla^2\Theta)^2|E|^2\Big]\sin^2\psi \\ &+2\nabla^2\Theta\,\nabla\Theta\cdot\nabla|E|^2\Big\}, \end{aligned} \tag{S12}$$

where we ignored terms of orders $(\zeta/k)^3$ and higher. Even the terms proportional to $(\zeta/k)^2$ can be dropped except when the analyzer angle is chosen so that the remaining two terms are very small. As was discussed in the main body, the optimal choice of $\psi$ is the one that makes the second term comparable to the first. By also measuring at $\psi = 0$ we can recover the first term to subtract it. In cases where the intensity is constant, this extra measurement is not necessary.

Finally, notice that the phase $\Phi_2$ can be ignored if, within the profile of the beam, it varies by an amount significantly smaller than $2\pi$. There are two parts to this phase, one that is independent of the incident beam's angular spectrum (i.e. the range of optical momenta $\boldsymbol{p}_0$), and one that depends on it. The first part gives us a condition for $\zeta$, which is that $k^{-2}\zeta^2\nabla\Theta\cdot\mathbb{H}_\Theta\cdot\nabla\Theta$ should vary in an amount significantly smaller than $2\pi$. This condition is automatically satisfied for a $\Lambda$-plate, and for a Geometric Phase Lens (GPL) it reduces to $\zeta \ll f^3/(\lambda r)$, where $f$ is the focal length of the lenses and $r$ is the radius of the beam. The second condition has two parts, but it is usually dominated by the first one, which can be written as $\zeta|\boldsymbol{p}_0\cdot\mathbb{H}_\Theta| \ll k$. This condition is satisfied if the range of the angular spectrum of the beam under test is much smaller than $(\lambda\zeta|\nabla^2\Theta|)^{-1}$. Again, for a $\Lambda$-plate this is automatically satisfied, while for a GPL it places a constraint on the level of collimation of the test beams, whose directional range should be smaller than $\lambda\zeta/f^2$.

## 2. EXAMPLES

The novelty of the proposed shearing mechanism via geometric phase objects is that it enables non-uniform shears, both in direction and magnitude. For the purpose of illustration, the shearing distance in the following examples is exaggerated by incrementing the propagation distance $\zeta$ between the SVAPs.

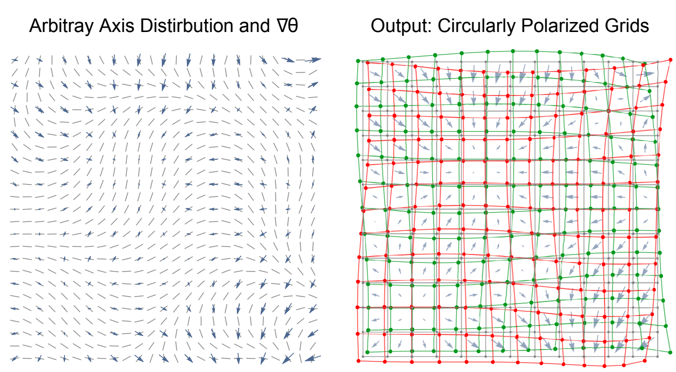


**Fig. S1.** (Left) General SVAP with arbitrary axis distribution $\Theta$. The blue arrows depict the gradient $\nabla\Theta$, which is proportional to the directional shifts that each circular component undergoes. (Right) Coordinate transformations undergone by both circular polarization components, shown in green and red, and the resulting local shearing $\boldsymbol{\epsilon}$ achieved via this mechanism, depicted by the light blue arrows. The original grid is shown in gray. The total shear is exaggerated for the sake of clarity.

Figure S1 illustrates the phase gradient caused by a generic SVAP with prescribed optical axis directions on circularly-polarized light. This causes that, after propagation through the second SVAP, the output left and right circularly polarized fields undergo opposite coordinate transformations, causing a spatially-varying shearing given by $\boldsymbol{\epsilon} = k^{-1}\zeta\nabla\Theta(\boldsymbol{x})$. Notice that the coordinate transformations for each circular polarization component may imply an expansion or contraction, whose effect is accounted for by the Jacobians $j_{\pm}$ (discussed in the previous section) to ensure power conservation.

Figure S2 shows the two cases discussed in the main body, corresponding to the use of Λ-plates and GPLs, which perform lateral and radial shears, respectively. Also shown is the case of Q-plates [1, 2], which perform a type azimuthal shear. Note that in this third case the central region of the grids is omitted. This is because, given the singularity at the centre of the SVAP, light near this region is scattered outwards given the large phase gradients. It can be easily seen that the direction mismatch given in Eq. (S6) for the Λ-plates is zero, whereas GPL's/Q-plates leave only/mainly a radial component having an opposite behavior for each handedness.

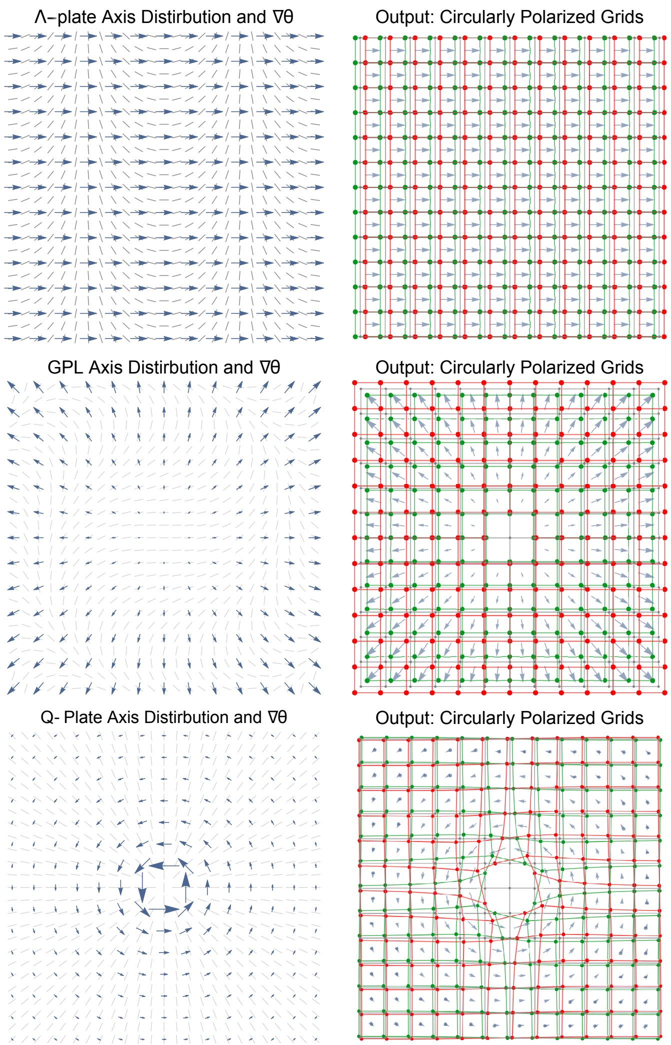


**Fig. S2.** (Left) SVAPs with simple geometries that lead to common shearing types. From top to bottom: lateral, radial and azimuthal shearing. Notice the opposite radial dependence of the magnitude of the gradient for Q-plates and GPLs: For GPLs the shearing vanishes linearly as one approaches the origin, while for Q-plates it diverges. (Right) Coordinate transformations for each circular polarization component, shown in green and red, and the resulting shearing distribution $\epsilon$ (depicted by the light blue arrows) achieved by each of these SVAP pairs. The original coordinates are shown in gray. The total shear is exaggerated for clarity.

## REFERENCES

1. B. Piccirillo, V. D'Ambrosio, S. Slussarenko1, L. Marrucci, and E. Santamato, Appl. Phys. Lett. **97**, 241104 (2010).
2. B. Piccirillo, S. Slussarenko1, L. Marrucci, and E. Santamato, Rivista del Nuovo Cimento **36**, 501–554 (2013).